BIOINFORMATION
Discovery at the interface of physical and biological sciences

open access www.bioinformation.net Hypothesis

Volume 9(20)

Model of β-Sheet of Muscle Fatty Acid Binding Protein of *Locusta migratoria* Displays Characteristic Topology

Nadeem A Kizilbash*, Abdul Hai & Jamal Alruwaili

Department of Biochemistry, Faculty of Medicine & Applied Medical Sciences, Northern Border University, Arar-91431, Saudi Arabia; Nadeem A. Kizilbash - Email: fsd707@gmail.com; Phone: +966-592390610; *Corresponding author

Received November 06, 2013; Accepted December 12, 2013; Published December 27, 2013

Abstract:
The β-sheet of muscle fatty acid binding protein of *Locusta migratoria* (*Lm*-FABP) was modeled by employing 2-D NMR data and the Rigid Body Assembly method. The model shows the β-sheet to comprise ten β-strands arranged anti-parallel to each other. There is a β-bulge between Ser 13 and Gln 14 which is a difference from the published structure of β-sheet of bovine heart Fatty Acid Binding Protein. Also, a hydrophobic patch consisting of Ile 45, Phe 51, Phe 64 and Phe 66 is present on the surface which is characteristic of most Fatty Acid Binding Proteins. A "gap" is present between β_D and β_E that provides evidence for the presence of a portal or opening between the polypeptide chains which allows ligand fatty acids to enter the protein cavity and bind to the protein.

Keywords: Muscle Fatty Acid Binding Protein, Nuclear Overhauser Effect, β-sheet of Lm-FABP, Portal hypothesis, *Locusta migratoria*.

Background:
In insects, body fat plays a major role **[1]**. Insects store lipids as glycogen and triglycerides in the adipocytes. The metabolism of lipids is important in insects for growth and reproduction and provides energy during non-feeding periods. In the resting locust, the major source of energy is Trehalose (a hemolymph) **[2]**. One advantage of using lipids as a source of energy is that they weigh less than isocaloric amounts of carbohydrates **[3, 4]**. The main storage form of lipids is as triglycerides which are released as diglycerides during flight **[4, 5]**.

Based on the tissue of origin, the intracellular fatty acid-binding proteins (FABPs) are divided into three categories: (i) hepatic-type FABPS, (ii) intestinal-type FABPS and (iii) muscle/cardiac-type FABPs. These proteins are 14-15 kDa in size and are important for the uptake, metabolism and transport of long-chain fatty acids. They are also responsible for the modulation of cell growth and proliferation. Human muscle and bovine heart fatty acid binding proteins bind long-chain fatty acids in the cytosol of muscle tissues.

According to the Portal hypothesis proposed for the uptake of fatty acids by FABPS, the fatty acid first adsorbs to the protein surface and then searches for an opening or portal by which it can enter the protein cavity. After finding the opening, the fatty acid enters the protein cavity. The next step is the protonation of the ligand, before de-solvation, which demands a large amount of energy (30 kJ mol^{-1}). Since the insertion of the negative charged ligand into the low dielectric matrix of the protein is energetically unfavorable, ligand-binding to the protein occurs before the protonation of the ligand. The insertion of the charged head-group of the ligand fatty acid inside the protein cavity requires energy in the amount of 300 kJ mol^{-1} **[6]**. Molecular dynamics simulations of I-FABP have

shown that the ligand first adsorbs to the protein surface. The rate limiting step is the de-solvation of the carboxylate head group of the fatty acid anion **[7]**.

The β-sheet of human muscle fatty acid binding protein displays ten β-strands arranged anti-parallel to each other in which each strand is hydrogen bonded to its neighbor. This arrangement is completed by the formation of hydrogen bonds between the first and the last β-strand **(Figure 1)**. The β-sheet is folded to form a β-barrel and contains an interior and an exterior surface. The interior surface serves as a cavity or a pit where the ligand binds **[8]**. The volume of this cavity varies between 300 and 700 Å^3 **[9]**. In this project, 2-D NMR data, specifically information provided by the Nuclear Overhauser Effect (NOE), was used to build a model of the β-sheet of *Lm*-FABP using the Rigid Body Assembly method and bovine heart FABP as a template **[10]**.

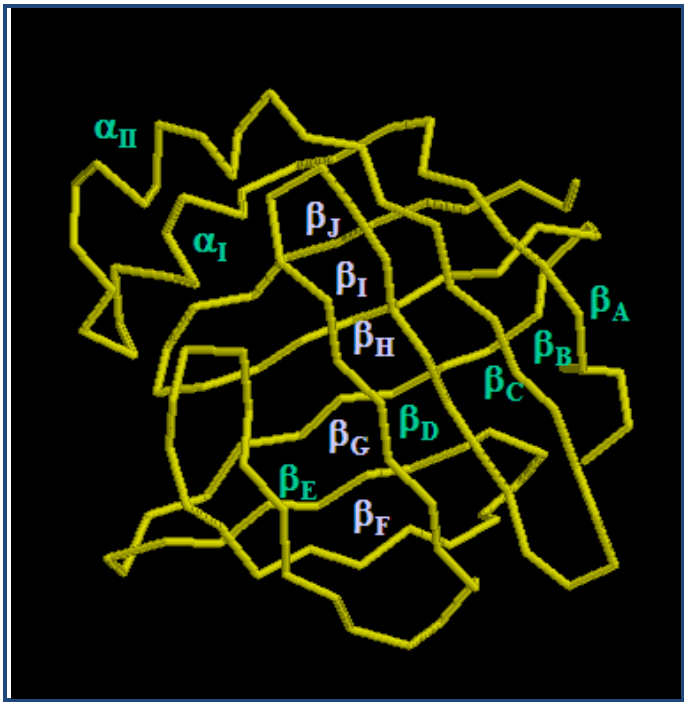

Figure 1: Backbone of human muscle FABP showing the arrangement of two α-helices (α_I and α_{II}) and ten β-strands (β_A, β_B, β_C, β_D, β_E, β_F, β_G, β_H, β_I and β_J) **[13]**.

Methodology:

The methodology used in the study is summarized in schematic 1 **(see supplementary material).**

Protein expression and purification

Lm-FABP was expressed in *E.coli* cells using previously published protocols **[11].** The cDNA of the protein was isolated after digestion with restriction endonucleases, NcoI and BamHI and ligated with the pET3d vector. The plasmid pET3d/*Lm*-FABP was used to transform the *E. coli* D12 strain BL21 (DE3) cells. Lm-FABP was purified by the use of previously published protocols **[11].** The protocol included cell lysis, centrifugation and purification by a Sepharose HR 26/10 FPLC column. *Lm*-FABP eluted with 50 mM Tris/HCl (pH 8.0). The fractions were analyzed by SDS/PAGE and Western blotting. Fractions containing *Lm*-FABP were further purified by gel filtration chromatography using a Sephacryl S-100 column.

NMR experiments

2-D homonuclear NMR spectra were acquired for protein sample bound to native fatty acids in 20 mM phosphate buffer (10% D_2O, 0.05% NaN_3) at pH 5.5 and 35 ^oC. These spectra were acquired in the "phase sensitive" mode with pre-saturation of the water signal to obtain maximum signal-to-noise ratio. All the chemical shifts were referenced with respect to sodium 3-(trimethylsilyl) [2,2,3,3-$^2H_4$] propionate (TSP). Once the spectra had been acquired, they were analyzed to assign chemical shifts and to collect NOE constraints that consist of sequential, medium range and long range constraints.

Amino Acid Sequence Alignment

Before analysis of the NMR data, the amino acid sequence of *Lm*-FABP was analyzed. The sequence is characterized by the presence of thirty one amino acids with aliphatic side chains. It also contains three Proline residues (Pro39, Pro91 & Pro103). The sequence also contains one Cysteine residue (Cys115). There are ten aromatic amino acid residues (seven Phenylalanines and three Tyrosines) and two Histidines (His102 and His96), also present in the sequence. In addition, the sequence is characterized by two Methionines, (f-Met 0 and Met 21).

A comparison of the sequence of *Lm*-FABP with the bovine heart FABP was performed using the FSSP data-base. The alignment revealed 42% sequence homology between two proteins. There are three insertions (Ile 7, Leu 46 and Asn 92) and two deletions (Gly 99 and Ala 132) in the sequence of *Lm*-FABP as compared to bovine heart FABP. The amino acid insertions are exactly the same if the sequence of *Lm*-FABP is compared to human muscle FABP. The only amino acid deleted is Gly 99.

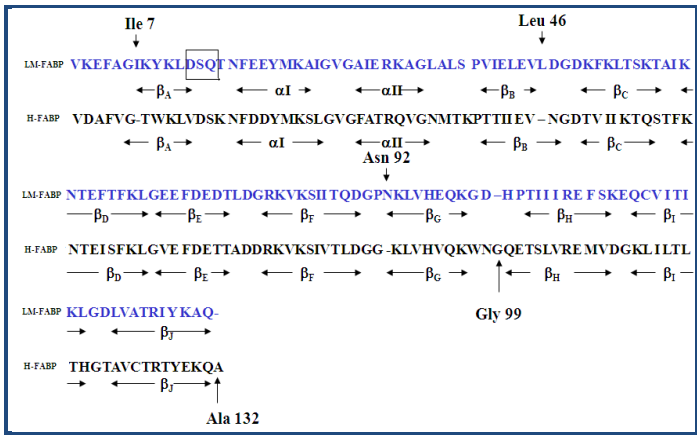

Figure 2: Comparison of secondary structure elements of *Lm*-FABP and bovine heart FABP showing the three insertions (Ile 7, Leu 46 and Asn 92) and the two deletions (Gly 99 and Ala 132).

Spin System Identification

2-D homonuclear COSY and TOCSY spectra were used to identify amino acid spin systems comprising J-coupled ^1H. The amide ^1H chemical shift dispersion in the 2-D TOCSY ranged from 10.18-6.78 ppm. The scalar coupled NH and $C_\alpha H$ ^1H were recognized in the "finger print" region of the 2-D COSY spectrum, as shown in **(Figure 2)**. To identify spin systems representing individual amino acids (comprising NH and $C_\alpha H$

along with the side-chains ^{1}H), the program AURELIA **[12]** was used to peak-pick the 2-D data. Initially, about 165 spin systems were identified. These included some doublets due to the presence of spin system heterogeneity. This list later was narrowed down to about 145 spin systems for 130 non-Proline amino acids in the protein. The three Proline residues present in the sequence were identified separately since they don't possess an amide ^{1}H.

NMR Chemical Shift Assignment

The strategy of sequential ^{1}H chemical shift assignment was followed to assign the backbone and side-chain NMR chemical shifts of *Lm*-FABP (data not shown).

Identification of Secondary Structure Elements

Secondary structure elements **(Figure 2)** were identified by characteristic Nuclear Overhauser Effect (NOE) cross-peaks as shown in schematic 2 **(see supplementary material).** The sequential NOEs observed for α-helices consist of a strong d_{NN} and a weak $d_{\alpha N}$ NOE cross-peak for each "i-1" and "i" amino acid residue. In addition to these medium range NOEs are also observed as shown in schematic. For β-strands, the characteristic NOE information is a strong $d_{\alpha N}$ and a weak d_{NN} cross-peak for "i-1" and "i" amino acid residues. For the β-turns, a strong-weak d_{NN} and strong to medium $d_{\alpha N}$ NOE crosspeaks are expected for "i-1" and "i" amino acid residues.

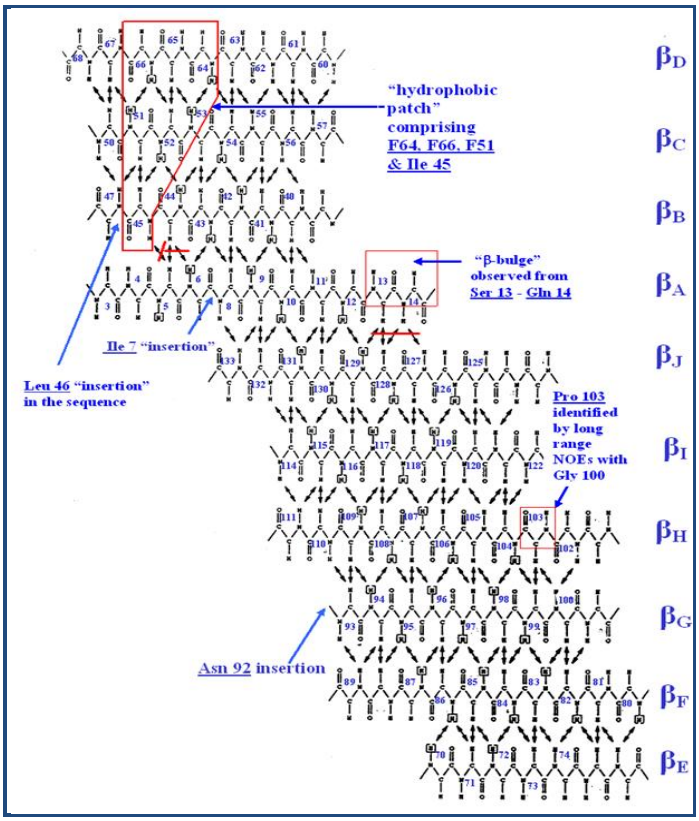

Figure 3: β-sheet of *Lm*-FABP modeled after bovine heart FABP by the use of 2-D NMR data and the Rigid Body Assembly method **[10]**.

Homology Modeling of β-sheet

The β-sheet of *Lm*-FABP **(Figure 3)** was modeled after the β-sheet of Bovine Heart FABP using the Rigid Body Assembly method **[10]**. This method starts with the identification of the conserved β-sheet of bovine H-FABP and then assembly of the model of β-sheet of *Lm*-FABP from the H-FABP template using the inter-strand NOE cross-peak intensities in **schematic 3, Table 1 (see supplementary material)**.

Discussion:

Many structures of human, bovine and insect FABPs are known via X-ray crystallography or NMR **[13-17].** These structures have provided details about ligand-binding property of FABPs. The FABPs display a ten-stranded β-sheet structure and a large, hydrophilic, water-filled inner cavity that serves as a ligand-binding site for hydrophobic ligands such as fatty acids and retinoids **[6].** The β-sheet of Lm-FABP shown in **(Figure 3)** closely resembles that of the other FABPs. The fatty acid is bound to FABPs by electrostatic and hydrogen bond interactions of its carboxylate head group with charged or polar residues inside the protein and by interactions of its tail with hydrophobic residues. A "gap" is observed between βD and βE in the β-sheet which can serve as a portal for entry of long chain fatty acids in the inner cavity of the protein.

A description of the ligand-binding process is given by the Portal hypothesis which describes the entry of long chain fatty acids inside the protein cavity through an opening or portal. The Portal hypothesis is supported by many experimental studies, most of which were carried out using either the I-FABP or ALBP. Crystallographic studies of both these proteins have indicated that the lipid tail is located near the suggested entry site **[18, 19].** NMR measurements of I-FABP have suggested that the protein exhibits a pronounced backbone disorder at the portal region and is more mobile than the rest of the protein suggesting that this region may be involved in ligand insertion **[17, 20, 21, 22]**.

Conclusion:

The information provided by the Nuclear Overhauled Effect was used to build a model of the β-sheet of *Lm*-FABP using the Rigid Body Assembly method and bovine heart FABP as a template. The β-sheet structure of *Lm*-FABP displays a typical structure of 10 anti-parallel β-strands arranged to form a sheet. A "gap" is observed between β_D and β_E. A β -bulge is also present between Ser 13 and Gln 14 which is a difference from the structure of bovine heart fatty acid binding protein. The observed "gap" between β_D and β_E provides evidence for the presence of a portal between the polypeptide chains which allows long chain fatty acids to enter the protein cavity and bind to the protein.

Acknowledgement:

We would like to thank HEJ Research Institute of Chemistry (Karachi, Pakistan) for the use of their 600 MHz NMR spectrometer.

References:

[1] Law JH & Wells MA, *J Biol Chem*. 1989 **264**: 16335 [PMID: 2674129]
[2] Weis-Fogh T, *Phil Trans R Soc (B)*. 1952 **237**: 1
[3] Beenakers AMT, *Insect Physiol*. 1965 **11**: 879
[4] Beenakers AMT, *Gen Camp Endocr*. 1969 **13**: 12
[5] Mayer RJ & Candy DJ, *Comp Biochem Physiol*. 1969 **31**: 409 [PMID: 5351972]

[6] Friedman R *et al. Biochemistry* 2005 **44**: 4275 [PMID: 15766256]
[7] Richieri GV *et al. J Biol Chem*. 1996 **271:** 11291 [PMID: 8626681]
[8] Veerkamp JH *et al. Biochim Biophys Acta*. 1991 **1081**: 1 [PMID: 1991151]
[9] Massolini G & Calleri E, *J Chromatogr B Analyt Technol Biomed Life Sci*. 2003 **797**: 255
[10] Marti-Renom MA *et al. Annu Rev Biophys Biomol Struct*. 2000 **29**: 291 [PMID: 10940251]
[11] Maatman RG *et al. Eur J Biochem*. 1994 **221:** 801 [PMID: 8174560]
[12] Gorler A *et al. J Magn Reson*. 1999 **137**: 39 [PMID: 10053131]
[13] Young ACM *et al. Structure* 1994 **2**: 523 [PMID: 7922029]
[14] Haunerland NH *et al. Biochemistry*. 1994 **33**: 12378 [PMID: 7918460]
[15] Lassen D *et al. Eur J Biochem*. 1995 **230**: 266 [PMID: 7601110]
[16] Zhang F *et al. J Biomol NMR*. 1996 **9:** 213 [PMID: 9204553]
[17] Lucke C *et al. Structure* 1996 **4:** 785 [PMID: 8805562]
[18] Sacchettini JC *et al. J Mol Biol*. 1989 **208**: 327 [PMID: 2671390]
[19] Xu Z *et al. J Biol Chem*. 1993 **268**: 7874 [PMID: 8463311]
[20] Hodsdon ME & Cistola DP, *Biochemistry* 1997 **36**: 2278 [PMID: 9047330]
[21] Hodsdon ME & Cistola DP, *Biochemistry 1997* **36:** 1450 [PMID: 9063893]
[22] Zhang FL *et al. Biochemistry* 2003 **42**: 7339 [PMID: 12809489]

Edited by P Kangueane
Citation: **Kizilbash *et al.*** Bioinformation 9(20): 1003-1009 (2013)

BIOINFORMATION

open access

Supplementary material:

Table 1: List of Nuclear Overhauser Effect (NOE) cross-peak intensities used for modeling of β-sheet of *Lm*-FABP after bovine heart FABP by the use of the Rigid Body Assembly method.

^{1}H Nuclei of Different Amino Acid Residues exhibiting Dipolar Interaction		Intensities of NOE Crosspeaks observed in 2-D NOESY spectrum
Ala 5 CαH	**Val 45 NH**	medium NOE
Ala 5 CαH	**Glu 44 CαH**	strong NOE
Gly 6 NH	**Glu 44 CαH**	medium NOE
Gly 6 NH	**Leu 43 NH**	weak NOE
Lys 8 CαH	**Leu 43 NH**	medium NOE
Lys 8 CαH	**Glu 42 CαH**	strong NOE
Ala 5 CαH	**Val 45 NH**	medium NOE
Ala 5 CαH	**Glu 44 CαH**	strong NOE
Gly 6 NH	**Glu 44 CαH**	medium NOE
Gly 6 NH	**Leu 43 NH**	weak NOE
Lys 8 NH	**Gln 133 NH**	weak NOE
Tyr 9 NH	**Glu 42 CαH**	medium NOE
Tyr 9 NH	**Ile 41 NH**	weak NOE
Tyr 9 CαH	**Ala 132 CαH**	strong NOE
Lys 8 NH	**Gln 133 NH**	weak NOE
Tyr 9 NH	**Glu 42 CαH**	medium NOE
Tyr 9 NH	**Ile 41 NH**	weak NOE
Tyr 9 CαH	**Ala 132 CαH**	strong NOE
Lys 10 CαH	**Ile 41 NH**	medium NOE
Lys 10 CαH	**Val 40 CαH**	strong NOE
Lys 10 NH	**Ala 132 CαH**	medium NOE
Lys 10 NH	**Lys 131 NH**	weak NOE
Leu11 NH	**Val 40 CαH**	medium NOE
Leu 11 CαH	**Lys 131 NH**	medium NOE
Leu 11 CαH	**Tyr 130 CαH**	strong NOE
Val 40 NH	**Lys 56 NH**	weak NOE
Ile 41 CαH	**Lys 56 NH**	medium NOE
Ile 41 CαH	**Ser 55 CαH**	strong NOE
Glu 42 NH	**Ser 55 CαH**	medium NOE
Glu 42 NH	**Thr 54 NH**	weak NOE
Leu 43CαH	**Thr 54 NH**	medium NOE
Leu 43CαH	**Leu 53 CαH**	strong NOE
Glu 44 NH	**Leu 53 CαH**	medium NOE
Glu 44 NH	**Lys 52 NH**	weak NOE
Val 45 CαH	**Lys 52 NH**	medium NOE
Val 45 CαH	**Phe 51 CαH**	strong NOE
Asp 47NH	**Phe 51 CαH**	medium NOE
Asp 47 NH	**Lys 50 NH**	weak NOE
Lys 50 CαH	**Leu 68 NH**	medium NOE
Lys 50 CαH	**Lys 67 CαH**	strong NOE
Phe 51 NH	**Lys 67 CαH**	medium NOE
Phe 51 NH	**Phe 66 NH**	weak NOE
Lys 52 CαH	**H Phe 66 NH**	medium NOE
Lys 52 CαH	**Thr 65 CαH**	strong NOE
Leu 53 NH	**Thr 65 CαH**	medium NOE
Leu 53 NH	**Phe 64 NH**	weak NOE
Thr 54 CαH	**Phe 64 NH**	medium NOE
Thr 54 CαH	**Glu 63 CαH**	strong NOE
Ser 55 NH	**Glu 63 CαH**	medium NOE
Ser 55 NH	**Thr 62 NH**	weak NOE
Lys 56 CαH	**Thr 62 NH**	medium NOE
Lys 56 CαH	**Asn 61 CαH**	strong NOE
Thr 57 NH	**Asn 61 CαH**	medium NOE
Thr 57 NH	**Lys 60 NH**	weak NOE
Glu 70 CαH	**Ile 86 NH**	medium NOE
Glu 71 NH	**Ile 86 NH**	weak NOE
Glu 71 NH	**Ile 85 CαH**	medium NOE
Phe 72 CαH	**Ile 85 CαH**	strong NOE
Phe 72 CαH	**Ser 84 NH**	medium NOE
Asp 73 NH	**Ser 84 NH**	weak NOE
Glu 71 NH	**Ile 85 CαH**	medium NOE

Phe 72 CαH	**Ile 85 CαH**	strong NOE
Phe 72 CαH	**Ser 84 NH**	medium NOE
Asp 73 NH	**Ser 84 NH**	weak NOE
Asp 73 NH	**Lys 83 CαH**	medium NOE
Glu 74 CαH	**Lys 83 CαH**	strong NOE
Glu 74 CαH	**Val 82 NH**	medium NOE
Val 82 CαH	**Asp 101 NH**	medium NOE
Val 82 CαH	**Gly 100 CαH**	strong NOE
Lys 83 NH	**Gly 100 CαH**	medium NOE
Lys 83 NH	**Lys 99 NH**	weak NOE
Ser 84 CαH	**Lys 99 NH**	medium NOE
Ser 84 CαH	**Gln 98 CαH**	strong NOE
Ile 85 NH	**Gln 98 CαH**	medium NOE
Ile 85 NH	**Glu 97 NH**	weak NOE
Ile 86 CαH	**Glu 97 NH**	medium NOE
Ile 86 CαH	**His 96 CαH**	strong NOE
Thr 87 NH	**His 96 CαH**	medium NOE
Thr 87 NH	**Val 95 NH**	weak NOE
Leu 94 NH	**Glu 109 CαH**	medium NOE
Leu 94 NH	**Arg 108 NH**	weak NOE
Val 95 CαH	**Arg 108 NH**	medium NOE
Val 95 CαH	**Ile 107 CαH**	strong NOE
His 96 NH	**Ile 107 CαH**	medium NOE
His 96 NH	**Ile 106 NH**	weak NOE
Glu 97 CαH	**Ile 106 NH**	medium NOE
Glu 97 CαH	**Ile 105 CαH**	strong NOE
Gln 98 NH	**Ile 105 CαH**	medium NOE
Gln 98 NH	**Thr 104 NH**	weak NOE
Lys 99 CαH	**Thr 104 NH**	medium NOE
Lys 99 CαH	**Pro 103 CαH**	strong NOE
Gly 100 NH	**Pro 103 CαH**	medium NOE
Gly 100 NH	**His 102 NH**	weak NOE
Thr 87 NH	**His 96 CαH**	medium NOE
Thr 87 NH	**Val 95 NH**	weak NOE
Leu 94 NH	**Glu 109 CαH**	medium NOE
Leu 94 NH	**Arg 108 NH**	weak NOE
Thr 104 CαH	**Gly 122 NH**	medium NOE
Ile 105 NH	**Lys 120 NH**	weak NOE
Ile 106 CαH	**Lys 120 NH**	medium NOE
Ile 106 CαH	**Ile 119 CαH**	strong NOE
Ile 107 NH	**Ile 119 CαH**	medium NOE
Ile 107 NH	**Thr 118 NH**	weak NOE
Arg 108 CαH	**Thr 118 NH**	medium NOE
Ile 107 NH	**Ile 119 CαH**	medium NOE
Arg 108 CαH	**Ile 117 CαH**	strong NOE
Glu 109 NH	**Ile 117 CαH**	medium NOE
Glu 109 NH	**Val 116 NH**	weak NOE
Phe 110 CαH	**Val 116 NH**	medium NOE
Phe 110 CαH	**Cys 115 CαH**	strong NOE
Ser 111 NH	**Cys 115 CαH**	medium NOE
Ser 111 NH	**Gln 114 NH**	weak NOE
Gln 114 CαH	**Ala 132 NH**	medium NOE
Gln 114 CαH	**Lys 131 CαH**	strong NOE
Cys 115 NH	**Lys 131 CαH**	medium NOE
Cys 115 NH	**Tyr 130 NH**	weak NOE
Val 116 CαH	**Tyr 130 NH**	medium NOE
Val 116 CαH	**Ile 129 CαH**	strong NOE
Ile 117 NH	**Ile 129 CαH**	medium NOE
Ile 117 NH	**Arg 128 NH**	weak NOE
Thr 118 CαH	**Arg 128 NH**	medium NOE
Thr 118 CαH	**Thr 127 CαH**	strong NOE
Ile 119 NH	**Thr 127 CαH**	medium NOE
Ile 119 NH	**Ala 126 NH**	weak NOE
Lys 120 CαH	**Ala 126 NH**	medium NOE
Lys 120 CαH	**Val 125 CαH**	strong NOE

*Intensity<60,000 = weak; Intensity <90,000 = medium; Intensity >90,000 = strong

*Intensities of NOE cross-peaks as observed in AURELIA peak-picked data.

ISSN 0973-2063 (online) 0973-8894 (print)
Bioinformation 9 (20):1003-1009 (2013)

Schematic 1: Methodology used for acquisition of NMR data and determination of the β-sheet.

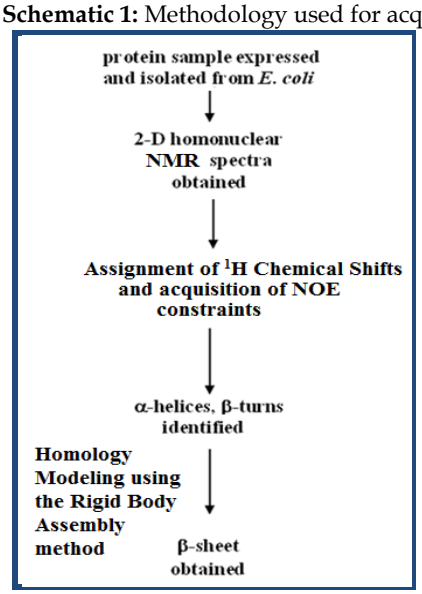

Schematic 2: Nuclear Overhauser Effect (NOE) cross-peak intensities used to identify -helices, β-strands and β-turns.

d_{NN} (i-1,i/i+1,i)	(2.4 Å)	strong NOE
$d_{\alpha N}$ (i-1,i)	(3.4 Å)	medium NOE
d_{NN} (i-2,i/i+2,i)	(4.2 Å)	weak NOE
$d_{\alpha N}$ (i-2,i)	(4.0 Å)	weak NOE
$d_{\alpha N}$ (i-3,i)	(3.4 Å)	medium NOE
$d_{\alpha N}$ (i-4,i)	(4.3 Å)	weak NOE
$d_{\beta\alpha}$ (i-3,i)	(3.5-5.0 Å)	medium-weak NOE

Sequential and medium range NOE cross-peaks observed for α-helices.

d_{NN} (i,i+1/i,i-1)	(4.5 Å)	weak NOE
$d_{N\alpha}$(i,i-1)	(2.2 Å)	strong NOE

Sequential (i,i+1/i,i-1) NOEs observed for β-strand.

type I β-turn

d_{NN} (residue 1,2/3,4)	(2.6 Å) strong NOE
d_{NN} (residue 2,3)	(2.4 Å) strong NOE
$d_{\alpha N}$ (residue 1,2/3,4)	(3.2 Å) medium NOE
$d_{\alpha N}$ (residue 3,4)	(3.4 Å) medium NOE

type II β-turn

d_{NN} (residue 1,2/3,4)	(2.4 Å) strong NOE
d_{NN} (residue 2,3)	(4.5 Å) weak NOE
$d_{\alpha N}$ (residue 1,2/3,4)	(3.2 Å) medium NOE
$d_{\alpha N}$ (residue 2,3)	(2.2 Å) strong NOE

Sequential NOE crosspeaks observed for β-turns.

Schematic 3: Inter-strand Nuclear Overhauser Effect (NOE) cross-peak intensities used for modeling of the β-sheet of *Lm*-FABP.

Sequential NOEs

d_{NN} (i,i+1/i,i-1)	4.5 Å	(weak NOE)
$d_{N\alpha}$(i,i-1)	2.2 Å	(strong NOE)

Inter-strand NOEs

d_{NN} (i,j)	3.3 Å (weak NOE)
$d_{N\alpha}$ (i,j)	3.2 Å (medium NOE)
$d_{\alpha\alpha}$ (i,j)	2.3 Å (strong NOE)

ISSN 0973-2063 (online) 0973-8894 (print)
Bioinformation 9 (20):1003-1009 (2013)